UDK 544.344.016.5:691.714.018.8
Original scientific article/Izvirni znanstveni članek

ISSN 1580-2949
MTAEC9, 56(1)51(2022)

MICROSTRUCTURE EVOLUTION OF CORRUGATED INTERFACE 304/Q345R ROLLING-COMPOSITE PLATE

RAZVOJ MIKROSTRUKTURE NA NAGUBANI MEJI V KOMPOZITNI PLOŠČI NASTALI Z VALJANJEM NERJAVNEGA JEKLA 304 IN JEKLA ZA TLAČNE POSODE Q345R

Guanghui Zhao[1,3,4], Ruifeng Zhang[1,3,4*], Juan Li[1,3,4], Huaying Li[1,3,4], Liu Haitao[2], Lifeng Ma[1,3,4]

[1]Taiyuan University of Science and Technology, Taiyuan 030024, China
[2]State Key Laboratory of Rolling and Automation, Northeastern University, Shenyang 110819, PR China
[3]Shanxi Provincial Key Laboratory of Metallurgical Device Design Theory and Technology
[4]The Coordinative Innovation Center of Taiyuan Heavy Machinery Equipment

Prejem rokopisa – received: 2021-10-12; sprejem za objavo – accepted for publication: 2021-12-10

doi:10.17222/mit.2021.291

A new method for the composite rolling of 304/Q345R was explored in the present study. The composite interface of the composite plate was studied using a scanning electron microscope (SEM) and electron-backscatter diffraction (EBSD). The results showed that a composite interface was formed with corrugated connections, increasing the length of the composite interface. Furthermore, the elongation of the corrugated interface relative to the original wave interface and the original horizontal interface were 29.43 % and 59.12 %, respectively. The composite interface became a 3D ripple interface from the traditional 2D plane. In the EBSD analysis, the strain energy at the interface of the corrugated composite interface was large, especially in the composite interface of the wave-waist position, indicating that the position of the ripple interface had a large deformation degree. This deformation is beneficial to the interface oxide and broken hardened layer conducive to the interface of the complex.

Key words: ripple interface, rolling composite, microstructure

V pričujočem članku avtorji predstavljajo novo metodo izdelave kompozita z medsebojnim valjanjem valovite plošče iz nerjavnega jekla vrste 304 in plošče iz jekla za tlačne posode Q345R. Medfazno mejo, nastalo na kompozitni plošči so analizirali z vrstičnim elektronskim mikroskopom (SEM) in difrakcijsko spektroskopijo na osnovi povratno sipanih elektronov (EBSD). Rezultati analiz so pokazali, da je kompozitna fazna meja nastala z gubanjem plasti jekla pri čemer se je povečala dolžina kompozitne meje. Nadalje je bilo podaljšanje z nagubanjem fazne meje v primerjavi z začetno stično mejo med obema ploščama jekla ocenjeno v horizontalni smeri za prvi izbrani primer 29,43 % oziroma za drugi primer 59,12 %. Nastala je tri-dimenzionalna (3D) nagrbančena (nagubana) fazna meja iz osnovne dvo-dimenzionalne (2D) plošče. EBSD analiza je pokazala, da je bila za nagubanje fazne meje potrebna velika deformacijska energija, še posebej v najožjem delu fazne meje kompozita. Na fazni meji je tako velika stopnja deformacije močno pripomogla k lomljenju trde površinske plasti jekla in drobljenju oksidov ter s tem do nastanka kompleksne kohezivne mejne površine kompozita, izdelanega iz plošč dveh različnih vrst jekla.

Ključne besede: nagubana mejna površina, valjanje kompozita, mikrostruktura

1 INTRODUCTION

Having carbon steel as the base layer and stainless steel cladding the composite panels, both the stainless steel's corrosion resistance and the carbon steel's mechanical strength and processing performance can be widely used in areas such as chemistry, marine engineering, construction, and food engineering.[1,2] As a material to save resources and reduce costs, it has aroused great interest and a variety of manufacturing methods have been developed, which can be mass-produced mainly through the rolling-composite method.[3,4]

In the 1980s, many researchers conducted research on metal solid-phase rolling compounds. For example, D. R. Cooper observed through scanning electron microscopy (SEM) that there were many oxide fragments on the metal-bonded surface of the composite plate, which was considered to be the interface between the two metals and the metal-bond connection of the layered metal.[5,6] L. Long underwent hot-rolled experimental studies of stainless steel and low-carbon steel.[7] The experimental results showed that there were impurities and oxides in the composite interface of the hot-rolled stainless-steel composite plate, and the distribution of the oxide layer was consistent with the distribution of the oxide layer in the N3-Bay metal solid-phase mechanism. The authors found that the coherence of the brittle layer at the interface of the composite metal broke during the rolling process, and fresh metal was exposed at the grassroots level and extruded from the fractured cracks in the brittle layer, which had been broken on both sides under the rolling pressure.[8,9] This mechanism was also confirmed by other researchers through SEM observations, though the composite interface's fracture-surface morphology

*Corresponding author's e-mail:
zrf18234222278@163.com (Ruifeng Zhang)

and the composition is yet to be confirmed.[10] In the past 5 years, researchers have carried out an in-depth study of a rolled stainless-steel composite panel, such as 304/Q235 clad plates. They obtained excellent properties, far exceeding the standards.[11–13]

However, for the existing production process of rolling clad plate, the rolling force required to achieve the composite state needs excellent requirements for the performance of the rolling mill. At the same time, the composite plate has the problem of a poor bonding strength and a low recombination rate due to the difference in the mechanical properties of the two kinds of metallic materials.[14,15] Furthermore, the composite interface is unstable and the toughness is poor.[16] Based on our previous understanding of the rolling-compounding mechanism, it was found that under the dual action of a strong rolling force and thermal diffusion, the compound surface-oxidation layer and the grinding-hardening layer of the two metals were broken. And the fresh metals of the substrate and the clad plate squeezed into each other under plastic deformation, Finally, metallurgical bonding was realized by hot-pressing diffusion The plastic deformation of the crack was crushed into the surface where there was contact. With the continuation of thermal pressure diffusion, the formation of the entire interface metal bond metallurgy was ultimately combined.[17,18] Based on the shortcomings of the current rolling-composite process, Wang Tao's research team first proposed the corrugated rolling-composite process. It had the characteristics of a low residual stress, a good plate shape and a high bonding strength.[19] They used the corrugated rolling method to roll an AZ31B magnesium alloy and a 5052 aluminum-alloy composite plate.[20] In the process of corrugated processing, the corrugated roller could accelerate the rupture of the substrate work-hardening layers and facilitate the mutual extrusion of fresh metals to enhance the interface bonding. Meanwhile, compared with the traditional flat-rolling method, the composite plate had a higher ultimate tensile strength of about 8 %.[21]

This paper presented a ripple interface rolling composite 304/Q345R composite board method. The composite interface of the composite plate was studied by using super-depth microscope (SEM), and electron-backscatter diffraction (EBSD) observations.

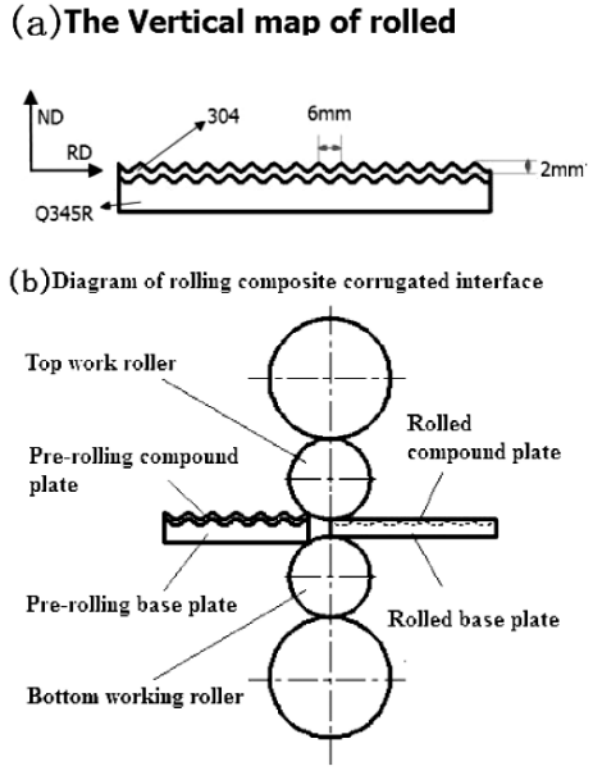

Figure 1: a) Corrugated slab side view, b) Diagram of rolling composite corrugated interface

2 EXPERIMENTAL PART

2.1 Materials

In this paper, the Q345R container steel composite board is used as the base layer, the 304 stainless steel is used as the compound layer, and the elemental composition of the base layer. The composite material is shown in **Table 1**.

Table 1: Chemical composition of clad and base materials (*w*/%)

	C	Si	Mn	P	S	Cr	Ni
304	0.04	0.33	1.37	0.037	0.005	18.3	8.1
Q345R	0.13	0.44	1.52	0.013	0.004	–	–

2.2 Experimental method

Based on the experimental conditions of the laboratory and the exploration of the riveting interface rolling process, the ripples in the test were machined with the wire-cutting method. The 304 stainless steel was placed parallel with the two sides of the corrugated plate, the Q345R container board was single corrugated (with stainless steel corresponding to the surface to be mixed), and the lower surface was flat. The specific shape of the corrugated billet is described in **Table 2**.

Using a wire brush wire-drawing machine to polish the substrate, the visible metal substrate was cleaned, the surface was polished with a wire brush to show the "sand surface" effect, and the roughness of the surface to be compounded was increased (conducive to the subsequent composite). The polished composite surfaces were cleaned with absolute ethanol to remove the adhesion and oil stain on the surface. Then the slab was dried and pressed. This was then followed by welding the composite slab with argon arc welding and a welding vacuum gas nozzle. Finally, two diffusion vacuum pumps were used on the slab vacuum using a 1×10^{-3} Pa high-vacuum state and a high-temperature hot-pressure-sealed suction nozzle. **Figure 1a** shows a side view of the corrugated slab. The composite slab was vacuum sealed, ordinary four-roll mill rolls were used for a flat roll

Table 2: Shape and dimensions of five kinds of corrugated plate (mm)

Waveform	304 thickness	Q345R average thickness	Wave height	Wave length	Plate length	Plate width	Total length of curve
2–6	3	9	2	6	100	100	122.9389

Table 3: Process table of corrugated hot rolling

Roll diameter (mm)	Rolling temperature (°C)	Rolling direction	Reduction rate (%)	Rolling speed (m/s)
306	1150	Vertical corrugation direction	25	0.2

through a pass, or rolled a number of times to meet the requirements of the thickness of the surface of the composite plate. The rolling diagram is shown in **Figure 1b**. The specific rolling process is presented in **Table 3**.

The microstructure of the composite interface of RD-ND was analyzed by line cutting and sampling on a 304/Q345R rolling composite plate, as shown in **Figure 2a**. A 4 % nitric acid alcohol etching solution was selected to erode the metallographic samples after erosion. The microscopic microstructures of the metal composite interface were observed with a Zeiss SIGMA SEM, and the elements were analyzed by scanning electron microscopy (SEM). The elemental analysis was carried out at the interface. The composite interface was analyzed by EBSD. The EBSD sample first underwent mechanical polishing and then electrolytic polishing. The electrolytic polishing liquid consisted of 10 % perchloric acid + 90 % acetic acid, was set at a voltage of 10 V, and a current of 0.16 A for 30–40 s. The EBSD interface with Channel5 software for deformation and orientation analysis.

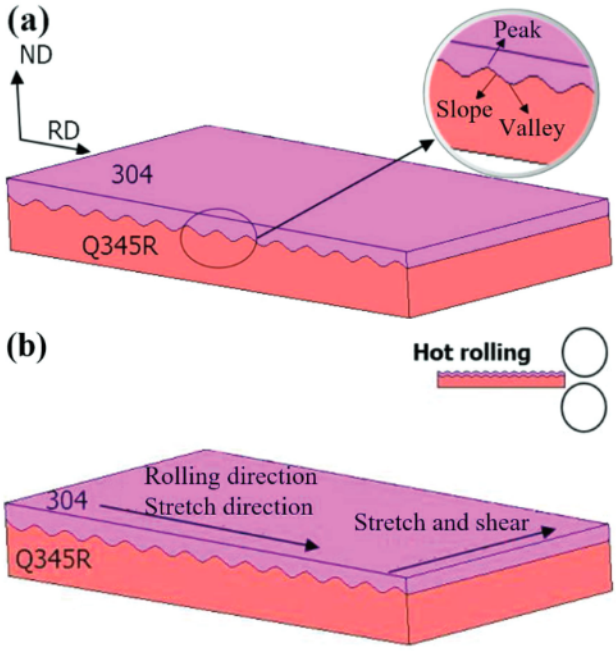

Figure 2: a) Location map of corrugated interface microstructure, b) Schematic view of hot-rolling process and test

3 RESULTS AND DISCUSSION

3.1 Composite interface morphology analysis

The composite plate produces plastic deformation under the action of high temperature and rolling pressure. It breaks the oxide layer on the contact surface of the two plates, and the atoms exposed on the fresh metal surface are embedded and attracted to each other. When the adjacent atoms are stably arranged, the outer free electrons of the two metal atoms form metal bonds, and the metal atoms diffuse to form a common diffusion layer and realize the recombination. When the adjacent atoms are arranged in a balanced pitch, the outer electrons of the two metal atoms become common electrons, forming metal bonds and adding metal atoms to each other to form a common diffusion layer. The composite deformation of the exposed surface exhibits one of the necessary conditions for the formation of welding nuclei. Another important factor in the formation of welding nuclei is the amount of pressure. Only a high enough pressure can produce a strong shear deformation and create more dislocation movement. Therefore, the deformation of the composite billet must be enough to promote the physical combination of components.[22] **Figure 3** shows the RD-ND cross-section composite effect of the composite sheet at a 25 % reduction in the waveform interface. As can be seen, for the upper part of the sample, the

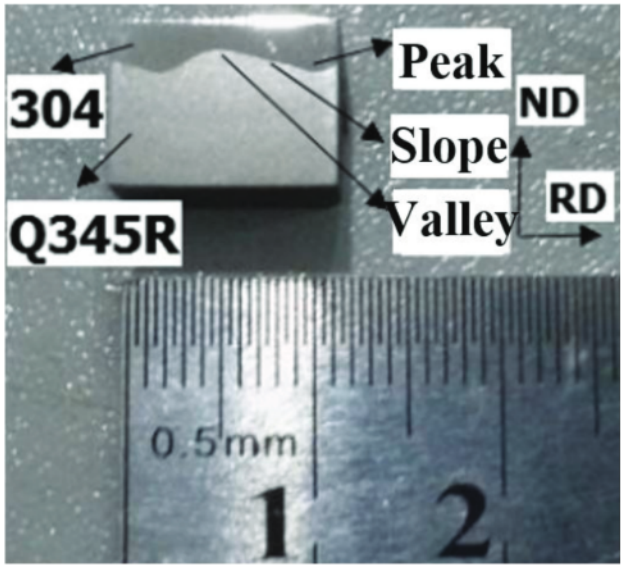

Figure 3: Location map of corrugated interface microstructure

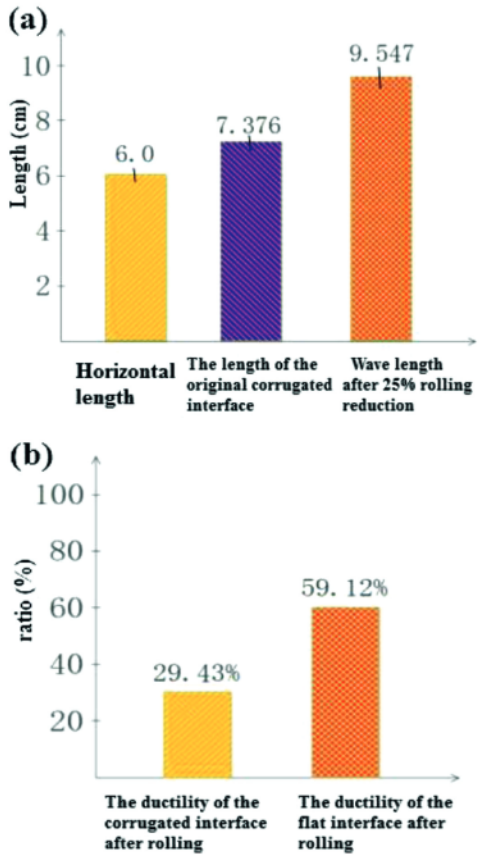

Figure 4: a) Interface length, b) relative elongation

color is bright 304 stainless steel, and the lower part of the color is dark Q345R container board, which forms a corrugated composite interface. It is then followed by the formation of the corrugated interface peaks and troughs. The ripple interface rolled 304/Q345R was rolled to form a 3D composite interface. The composite plate was subjected to ultrasonic flaw detection, and the composite ratio was 100 %.

Figure 4a presents the measured interface length. The corrugation length before and after rolling is 7.376 mm and 9.547 mm, respectively, and the horizontal length of the ripple is 6 mm. The ripple interface clearly increases the area of the interface between the 304 stainless steel and Q345R steel. **Figure 4b** shows the rate of the original wave interface and the original horizontal interface of the corrugated interface, which are 29.43 % and 59.12 %, respectively. The interfacial rolling increases the ductility of the composite interface, allowing the flat interface to increase more obviously. From the above analysis it can be seen that the ripple interface helps to increase the ductility of the composite interface, which is beneficial for the recombination. X. Li, from the China University of Science and Technology, studied aluminum/dovetail channel explosion welding to enhance the composite plate bonding rate and increase the interface area, and studied the composite interface of the meshing connection structure of the composite plate to increase the composite area and improve the quality of the composite.[23,24]

3.2 Composite interface microstructure analysis

Figures 5a to **5c** correspond to a 25 % reduction rate of the composite interface peak, wave waist, and trough position. It can be seen from **Figure 5** that, under the

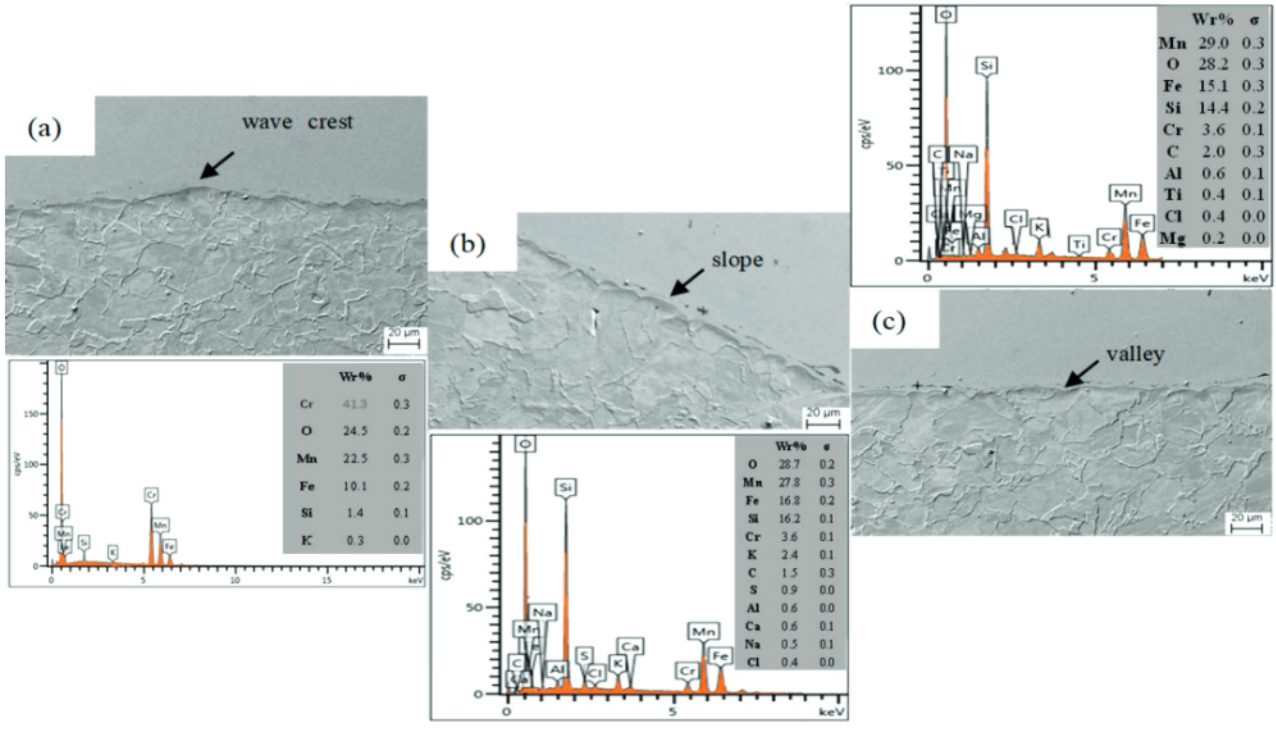

Figure 5: The 1000× SEM photos and EDS results: a) wave crest, b) slope, c) valley

wave depth of 2 mm, wavelength of 6 mm, and 25 % reduction rate, the grains at the wave crest of the composite interface are the smallest, which is then followed by the valley, and the wave waist have mixed crystals, where the grain size is uneven. This is due to the actual reduction rate of the peak. There are more impurities and oxides at the composite interface wave waist position, which shows a 10–20-μm-long strip along the interface distribution. Furthermore, the peaks and valleys at the composite interface are relatively clean, the particles of the impurities and oxides are small, and the peak at the actual reduction rate is conducive to breaking the metal having a complex interface with the contaminants and oxide layer, causing the fresh metal in the larger rolling to be under the control of the metallurgical compound. Due to the contact deformation of the corrugated interface, the interface of the composite interface is also relatively clean, which increases the relative shear movement deformation of the interface metal structure. This is beneficial to the interface friction, enhances the interface "cracking and embedding", and promotes the surface-hardening layer, accelerated membrane rupture, and dislocation. Under the action of thermal diffusion, the composite interface at the trough can achieve suitable recombination by hot-pressure diffusion. There are also fewer local oxide particles and composite interface impurities and oxides at the wave waist position. Due to the large actual reduction rate at the wave crest, it is conducive to crush the polluted layer and oxide layer at the interface to be compounded, so that the fresh metal can produce metallurgical compounding under a large rolling force. The black impurities and oxides at the composite interface were analyzed by EDS. The main elements at the wave crest of the composite interface are Fe, Cr, Mn and O from Cr and Mn oxides. Mn and Si oxides are mainly contained at the slope of the composite interface. The valley of the composite interface mainly contains Mn and Si oxides.

Figure 6 shows a wave with a depth of 2 mm and wavelength of 6 mm, and a 25 % reduction rate of the composite interface scan-line results. **Figure 6a** to **6c** correspondingly shows the line-scan results of the composite interface peak, wave waist, and trough position at a 25 % reduction rate. The Fe, Cr, and Ni greatly change at the wavelength of 6 mm and a 25 % reduction in the wave depth. This is because the difference between Fe, Cr, and Ni in the Q345R substrate is obvious. The 304 stainless steel contains a significant amount of Cr and Ni, and a relatively small amount of Fe. Furthermore, the energy spectrum of C and other light elements' sensitivity is low, so the change in the composite interface on both sides of the C element is not obvious. The 304 stainless steel in the Cr and Ni cross the original interface to the carbon steel side of the diffusion, and the Cr diffusion distance is higher than that for the Ni. The diffusion of the composite interface elements from the diffusion layer of Cr and Ni, and the element diffusion layer at the wavefront, wave waist, and trough at the composite interface is approximately (13; 19; 15) μm, respectively.

3.3 EBSD analysis

The composite interface of the corrugated interface 304/Q345R composite plate with a wave depth of 2 mm and wavelength of 6 mm was studied. The EBSD technique was used to study the composite interface's orientation, dynamic recrystallization and strain energy.

Figure 7 presents the plane of the ripple interface at a 25 % reduction rate of the composite interface (IPF) + grain boundary, where the RD and ND directions are selected. For the upper half of the composite interface, the fine grain is Q345R container steel, the middle of the white is not resolved out of the composite interface transition layer, and the lower part is 304 stainless steel. It can be seen from **Figure 8** that the corrugated interface Q345R steel side of the grain is small, and the changes in the crest, wave waist, and trough are not obvious. Additionally, there is no obvious preferred orientation. The 304 stainless-steel side grain is not uniform, there is no obvious preferred orientation at the peak position of the smallest grain, and the wave waist and trough position have coarse grains. Each large grain shows an orientation, where there are few color differences near the grain boundary. In other words, the grain boundary near the orientation subtly changes, and the grains at the wave valley are relatively smaller than those at the wave waist. For the corrugated interface of the 304 stainless-steel side, the wave waist and trough position of the large

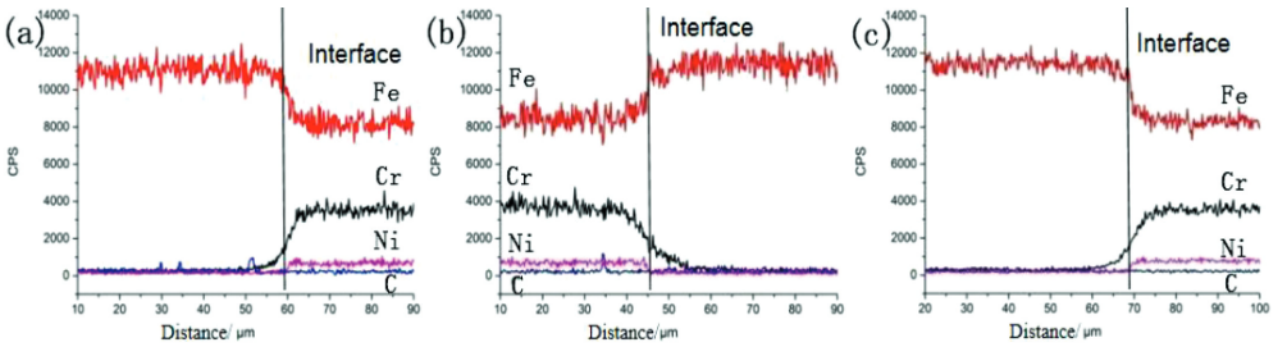

Figure 6: Results of SEM: a) wave crest, b) slope, c) valley

crystal grain is attributable to the observation and analysis of the corrugated interface on the role of stainless steel showing difficulty in changing the metal. The billet selection of the coarse grain and the stainless-steel grain are thick. The actual rolling temperature is approximately 1150 °C, and the grain grows rapidly.

Figure 8 shows a wave with a wave depth of 2 mm and wavelength of 6 mm ripple interface rolling composite interface orientation difference (local mis-orientation), which reflects the degree of deformation of the composite interface. Each composite interface of the reverse pole of the upper part of the fine grain is Q345R container steel, the middle of the white is not resolved out of the composite interface transition layer, and the lower part is 304 stainless steel. It can be seen from **Figure 8** that there is a uniform orientation difference distribution on the steel side of the corrugated interface Q345R, indicating that the degree of deformation is relatively consistent. Furthermore, at the 304 stainless-steel side of the ripple interface, the apparent orientation difference is mainly distributed at the composite interface. On the grain boundary of the composite interface and large grains, a large deformation can be observed. At the 25 % reduction rate, there is a significant difference in the orientation of the composite interface at the waist position, indicating that the position of the corrugated interface wave waist has a large degree of deformation. This deformation facilitates the breakage of the interface oxide and the hardened layer of the compound.

4 CONCLUSIONS

1) The corrugated interfacial rolling composite 304/Q345R rolling composite method was used to form a composite surface that exhibits a corrugated shape. Not only does it increase the length of the composite interface, but the composite interface from the traditional 2D plane also becomes a 3D ripple interface.

2) With a wave depth of 2 mm and wavelength of 6 mm, there is a 25 % reduction rate of the composite interface peak at the smallest grain, which is followed by the valley at the grain. The wave waist at a certain degree of mixed crystal grain size is not uniform. The contact deformation of the interfacial interface increases the number of intertwined metal structures relative to the shear deformation, facilitating interface friction, enhancing the interface "rupture and embedding", promoting the surface-hardening layer, and accelerating the rupture of the oxide film.

3) The diffusion of the complex interface elements forms the diffusion layer of Cr and Ni, and the element diffusion layer at the composite interface is about (13; 19; 15) μm, respectively. In the EBSD analysis, the strain energy at the interface of the corrugated composite interface is large, especially in the composite interface of the wave-waist position, which indicates that the position of the ripple interface has a large deformation degree.

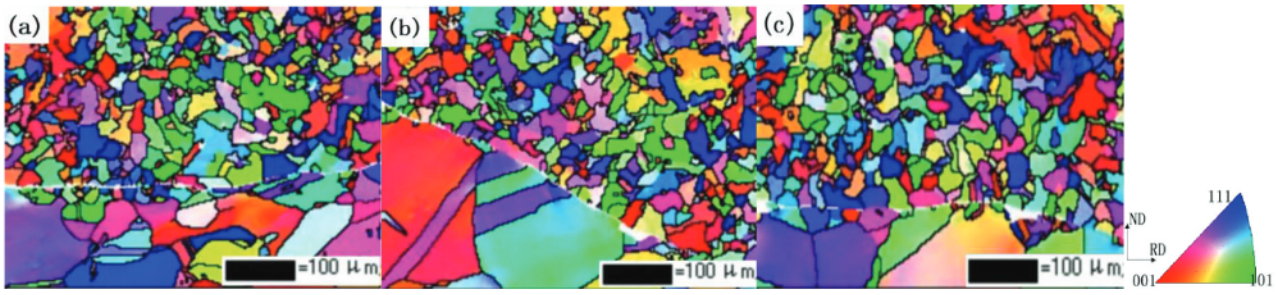

Figure 7: Reconstructed maps using IPF contrast for composite plate with corrugated interface under 25 % rolling rate: a) wave crest, b) slope, c) valley

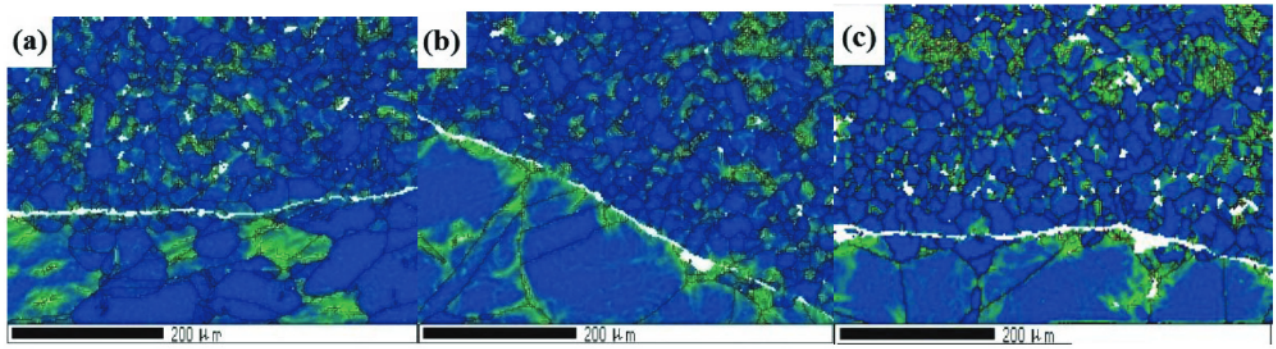

Figure 8: Reconstructed maps using local mis-orientation for a roll-bonded 304/Q345R composite plate with a 2–6 corrugated interface: a) wave crest, b) slope, c) valley

Acknowledgment

This project was supported by the National Key Research and Development Program of China (2018YFA0707305), the Science and Technology Major Project of Shanxi Province (20181101015), the Shanxi Outstanding Doctorate Award Funding Fund (20182061), the Scientific and Technological Innovation Programs of Higher Education Institutions in Shanxi (2019L0622), Natural Science Foundation of Liao-ning Province (No.2019-KF-25-05), Taiyuan University of Science and Technology doctoral Research Startup Fund (20212026), and the Coordinative Innovation Center of Taiyuan Heavy Machinery Equipment.

Declaration

The authors declare no conflict of interest.

5 REFERENCES

[1] Q. Zhang, S. Li, J. Liu, Y. Wang, B. Zhang, L. Zhang, Study of a bimetallic interfacial bonding process based on ultrasonic quantitative evaluation, Metals, 8 (**2018**), 329, doi:10.3390/met8050329

[2] Z. Dhib, N. Guermazi, M. Gaspérini, N. Haddar, Cladding of low-carbon steel to austenitic stainless steel by hot-roll bonding: microstructure and mechanical properties before and after welding. Maters. Sci. and Eng. A, 656 (**2016**), 130–141, doi:10.1016/j.msea.2015.12.088

[3] Z. Zhao, N. Tariq, J. Tang, Y. Ren, H. Liu, M. Tong, L. Yin, H. Du, J. Wang, T. Xiong, Influence of annealing on the microstructure and mechanical properties of Ti/steel clad plates fabricated via cold spray additive manufacturing and hot-rolling, Maters. Sci. and Eng., 775 (**2020**), 2147–2152, doi:10.1016/j.msea.2020.138968Jiang

[4] Y. Chao, F. Lun, X. Hong, L. Qiang, B. Bga, Effect of carbon content on the microstructure and bonding properties of hot-rolling pure titanium clad carbon steel plates, Maters. Sci. and Eng. A, 820 (**2021**), 141572, doi:10.1016/j.msea.2021.141572

[5] D. R. Cooper, J. M. Allwood, Influence of Diffusion Mechanisms in Aluminium Solid-state Welding Processes, Procedia Eng., 81 (**2014**), doi:10.1016/j.proeng.2014.10.300

[6] B. Xie, M. Sun, B. Xu, C. Wang, D. Li, Y. Li, Dissolution and evolution of interfacial oxides improving the mechanical properties of solid state bonding joints, Maters. and Des., 157 (**2018**), 437–446. doi:10.1016/j.matdes.2018.08.003

[7] L. Long, Z. Xinjin, Z. Zhichao, L. Huiyun, Investigation on bonding of stainless steel clad plate by vacuum hot rolling, Jour. of Mater. and Metal., 13 (**2014**), 48–49

[8] B-B. Zhou, C-Y. Zhou, L. Chang, X-C. Yu, C. Ye, B. Zhang Investigation on fatigue crack growth behavior of Zr702/TA2/Q345R explosive welding composite plate with a through-wall crack, Composite structures, 236 (**2020**), doi:10.1016/j.compstruct.2019.111845

[9] K. Geng, Y. Li, Z. Chu, Z. Ding, S. Wang, Study on characteristics of rolling process for stainless steel composite plate, Forging and stamping technology, 44 (**2019**), 34–42

[10] M. Eizadjou, H. D. Manesh, K. Janghorban, Investigation of roll bonding between aluminum alloy strips, Maters and Des., 29 (**2008**), 909–913, doi:10.1016/j.matdes

[11] F. Findik, Recent developments in explosive welding, Maters. and Des., 32 (**2011**), 1081–1093, doi:10.1016/j.matdes

[12] D. H. Yang, Z. A. Luo, G. M. Xie, M. K. Wang, R. D. K. Misra, Effect of vacuum level on microstructure and mechanical properties of titanium–steel vacuum roll clad plates, Journal of Iron & Steel Research International, 25 (**2018**), 72–80. doi:10.1007/s42243-017-0009-8

[13] D. H. Yang, Z. A. Luo, G. M. Xie, T. Jiang, S. Zhao, R. D. K. Misra, Interfacial microstructure and properties of a vacuum roll-cladding titanium-steel clad plate with a nickel interlayer, Maters. Sci. and Eng. A, 753 (**2019**), 49–58, doi:10.1016/j.msea.2019.03.008

[14] R. V. Kumar, R. Keshavamurthy, C. S. Perugu, P. G. Koppad, M. Alipour, Influence of Hot Rolling on Microstructure and Mechanical Behaviour of Al6061-ZrB2 In-situ Metal Matrix Composites, Maters. Sci. and Eng. A, 738 (**2018**), doi:10.1016/j.msea.2018.09.104

[15] L. Z. Wang, Study on Microstructure and Mechanical Properties of Explosive Welding Composite Plate, Key Eng. Maters., 723 (**2016**), 258–261, doi:10.4028/www.scientific.net/KEM.723.258

[16] S. Wang, G. Zhao, Y. Li, J. Li, Y. Song, Composite Plate Rolling Technology of 304/Q345R Based on a Corrugated Interface, Materials, 12 (**2019**), 3866, doi:10.3390/ma12233866

[17] G. Zhao, Q. Huang, C. Zhou, X. G. Wang, C. L. Zhou, Experiment and simulation analysis of roll-bonded Q235 steel plate, Revista De Metalurgia, 52 (**2016**) 2, 1–9, doi:10.3989/REVMETALM.069

[18] G. Zhao, Q. Huang, Z. Zhang, C. Zhou, M. A. Lifeng, Research on Microstructure and Mechanical Properties of Rolling Cladding Q235B Extra Thick Steel Plate, Hot working tech., 13 (**2016**), 1–4, doi:10.14158/j.cnki.1001-3814.2016.13.001

[19] W. Tao, Q. Yanyang, L. Jianglin, Research progress of rolling composite process of metal laminates at home and abroad, Jour. of Harbin University of tech., 52 (**2020**), 15, doi:10.1007/s40430-020-02626-6

[20] S. Li, J. Han, T. Wang, Y. Liu, J. Liu, Interfacial evolution and mechanical property of AZ31bmg/5052Al clad plate manufactured by corrugated + flat rolling technique, Procedia Manufacturing, 50 (**2020**), 148–152, doi:10.1016/j.promfg.2020.08.028

[21] X. Guo, Z. Ren, X. Ma, Effect of temperature and reduction ratio on the interface bonding properties of TC4/304 plates manufactured by EA rolling, Jour. of Manu. Pro., 64 (**2021**), 664–673, doi:10.1016/j.jmapro.2021.02.006

[22] L. Jiyuan, Research on deformation rules of Heavy Gauge Steel Plate clad rolling, Shenyang, Northeastern, 31 (**2010**), 23–36, doi:10.11181/hpi1972.31.343

[23] X-J. Li, H-H. Ma, Z-W. Shen, G-H. Miu, Explosive Welding of Aluminum-steel of Dovetail Groov, Chinese jour of energy. Maters., 24 (**2016**), 188–193, doi:10.11943/j.issn.1006-9941.2016.02.014

[24] X. Li, Reseach on Interface Effect and bonding mechanism of explosively clad plate with groove interface, University of Sci and Tech. of China, 16 (**2016**), 13–36, doi:10.1166/jnn.2016.12704